Some Computer Assisted Proofs for Solutions of the Heat Convection Problems (Theoretical development and feasibility of mathematical analysis on the computer)

AUTHOR(S):

Watanabe, Yoshitaka; Nakao, Mitsuhiro T.; Yamamoto, Nobito; Nishida, Takaaki

数理解析研究所講究録 1286 巻 2002 年 17-26

熱対流問題の解に対する計算機援用証明

Some Computer Assisted Proofs for Solutions of the Heat Convection Problems

渡部 善隆 † Yoshitaka Watanabe　　中尾 充宏 ‡ Mitsuhiro T.Nakao　　山本 野人 * Nobito Yamamoto　　西田 孝明 * Takaaki Nishida

† 九州大学情報基盤センター　‡ 九州大学大学院数理学研究院

* 電気通信大学情報工学科　* 京都大学大学院理学研究科

概 要

This is a continuation of our previous results [7]. In [7], the authors considered the two-dimensional Rayleigh-Bénard convection and proposed an approach to prove the exsistence of the steady-state solutions based on the infinite dimensional fixed-point theorem using Newton-like operator with the spectral approximation and the constructive error estimates. We numerically verified several exact non-trivial solutions which correspond to the bifurcated solutions from the trivial solution. This paper shows more detailed results of verification for the given Prandtl and Rayleigh numbers, which enables us to study the global bifurcation structure. All numerical examples discussed are taken into account of the effects of rounding errors in the floating point computations.

1 The Rayleigh-Bénard Problems

Consider a plane horizontal layer ($0 \leq z \leq h$) of an incompressible viscous fluid heated from below. At the lower boundary: $z = 0$ the layer of fluid is maintained at temperature $T + \delta T$ and the temperature of the upper boundary ($z = h$) is T (see Fig.1).

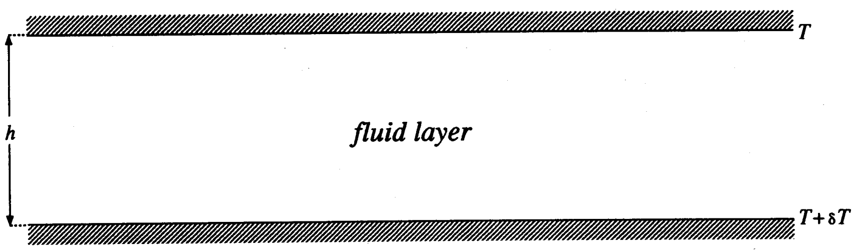

Fig.1. Geometry of the convection problem.

All variations with respect to y-direction are assumed to vanish, then according to the Oberbeck-Boussinesq approximations [1, 3], the equations governing convection in a layer in the two-dimensional (x-z) are described as follows:

$$\left\{\begin{array}{rcl} u_t + uu_x + wu_z & = & -p_x/\rho_0 + \nu\Delta u, \\ w_t + uw_x + ww_z & = & -(p_z + g\rho)/\rho_0 + \nu\Delta w, \\ u_x + w_z & = & 0, \\ \theta_t + u\theta_x + w\theta_z & = & \kappa\Delta\theta. \end{array}\right. \tag{1}$$

In the above system (1), $(u, 0, w)$ is the velocity vector field in the respective direction (x, y, z); p is the pressure field; θ is the temperature; ρ is the fluid density; ρ_0 is the density at temperature $T + \delta T$; ν is the kinematic viscosity; g is the gravitational acceleration; κ is the coefficient of thermal diffusivity; $*_\xi := \partial/\partial\xi (\xi = x, z, t)$; and $\Delta := \partial^2/\partial x^2 + \partial^2/\partial z^2$. The Oberbeck-Boussinesq approximation also requires that the fluid density is to be independent of pressure and depends linearly on the temperature θ, therefore ρ can be represented by

$$\rho - \rho_0 = -\rho_0 \alpha(\theta - T - \delta T),$$

where α is the coefficient of thermal expansion.

The Oberbeck-Boussinesq equations (1) have a stationary solution:

$$u^* = 0, \quad w^* = 0, \quad \theta^* = T + \delta T - \frac{\delta T}{h} z, \quad p^* = p_0 - g\rho_0 (z + \frac{\alpha \delta T}{2h} z^2)$$

representing the purely heat conducting state, where p_0 is a constant. By setting

$$\hat{u} := u, \qquad \hat{w} := w, \qquad \hat{\theta} := \theta^* - \theta, \qquad \hat{p} := p^* - p,$$

the perturbed equations:

$$\left\{ \begin{array}{rcl} \hat{u}_t + \hat{u}\hat{u}_x + \hat{w}\hat{u}_z & = & \hat{p}_x/\rho_0 + \nu\Delta\hat{u}, \\ \hat{w}_t + \hat{u}\hat{w}_x + \hat{w}\hat{w}_z & = & \hat{p}_z/\rho_0 - g\alpha\hat{\theta} + \nu\Delta\hat{w}, \\ \hat{u}_x + \hat{w}_z & = & 0, \\ \hat{\theta}_t + \delta T\hat{w}/h + \hat{u}\hat{\theta}_x + \hat{w}\hat{\theta}_z & = & \kappa\Delta\hat{\theta}, \end{array} \right. \tag{2}$$

are obtained. Moreover, transforming to dimensionless variables:

$$t \to \kappa t, \quad u \to \hat{u}/\kappa, \quad w \to \hat{w}/\kappa, \quad \theta \to \hat{\theta}h/\delta T, \quad p \to \hat{p}/(\rho_0\kappa^2)$$

of (2), the dimensionless equations:

$$\left\{ \begin{array}{rcl} u_t + uu_x + wu_z & = & p_x + \mathcal{P}\Delta u, \\ w_t + uw_x + ww_z & = & p_z - \mathcal{P}\mathcal{R}\,\theta + \mathcal{P}\Delta w, \\ u_x + w_z & = & 0, \\ \theta_t + w + u\theta_x + w\theta_z & = & \Delta\theta \end{array} \right. \tag{3}$$

are led, where

$$\mathcal{R} := \frac{\delta T \alpha g}{\kappa \nu h}$$

is the Rayleigh number[1] and

$$\mathcal{P} := \frac{\nu}{\kappa}$$

is the Prandtl number.

[1]The Rayleigh number is sometimes defined by $\mathcal{R} = (\delta T \alpha g h^3)/(\kappa\nu)$ when the dimensionless equations are reduced to the domain of $0 \le z \le 1$.

2 A fixed-point formulation

We shall find the *steady-state solutions*, u_t, w_t and θ_t are equated to 0 in (3), and assume that all fluid motion is confined to the rectangular region $\Omega := \{0 < x < 2\pi/a,\ 0 < z < \pi\}$ for a given wave number $a > 0$. Let us impose periodic boundary condition (period $2\pi/a$) in the horizontal direction, stress-free boundary conditions ($u_z = w = 0$) for the velocity field and Dirichlet boundary conditions ($\theta = 0$) for the temperature field on the surfaces $z = 0, \pi$, respectively. Furthermore, we assume the following evenness and oddness conditions:

$$u(x,z) = -u(-x,z), \quad w(x,z) = w(-x,z), \quad \theta(x,z) = \theta(-x,z).$$

We introduce the stream function Ψ, through the definition

$$u = -\Psi_z, \quad w = \Psi_x$$

so that $u_x + w_z = 0$. Cross-differentiating the equation of motion in (3) in order to eliminate the pressure p and setting $\Theta := \sqrt{\mathcal{PR}}\theta$, we obtain

$$\left\{\begin{array}{rcll} \mathcal{P}\Delta^2\Psi &=& \sqrt{\mathcal{PR}}\,\Theta_x - \Psi_z\Delta\Psi_x + \Psi_x\Delta\Psi_z & \text{in } \Omega, \\ -\Delta\Theta &=& -\sqrt{\mathcal{PR}}\,\Psi_x + \Psi_z\Theta_x - \Psi_x\Theta_z & \text{in } \Omega. \end{array}\right. \tag{4}$$

From the boundary conditions imposed above, the stream function Ψ and departure of temperature from linear profile Θ can be represented by the following double Fourier series:

$$\Psi = \sum_{m=1}^{\infty}\sum_{n=1}^{\infty} A_{mn}\sin(amx)\sin(nz), \quad \Theta = \sum_{m=0}^{\infty}\sum_{n=1}^{\infty} B_{mn}\cos(amx)\sin(nz). \tag{5}$$

By (5), we introduce following function spaces for $k \geq 0$:

$$X^k := \left\{\Psi = \sum_{m=1}^{\infty}\sum_{n=1}^{\infty} A_{mn}\sin(amx)\sin(nz) \mid A_{mn} \in \boldsymbol{R}, \right.$$
$$\left. \sum_{m=1}^{\infty}\sum_{n=1}^{\infty}((am)^{2k} + n^{2k})A_{mn}^2 < \infty\right\},$$

$$Y^k := \left\{\Theta = \sum_{m=0}^{\infty}\sum_{n=1}^{\infty} B_{mn}\cos(amx)\sin(nz) \mid B_{mn} \in \boldsymbol{R}, \right.$$
$$\left. \sum_{m=0}^{\infty}\sum_{n=1}^{\infty}((am)^{2k} + n^{2k})B_{mn}^2 < \infty\right\}$$

which are considered as closed subspaces of usual k-th order Sobolev space $H^k(\Omega)$.

For $M_1, N_1, M_2 \geq 1$ and $N_2 \geq 0$, we indicate a relation $N := (M_1, N_1, M_2, N_2)$ and define the finite dimensional approximate subspaces by

$$\begin{aligned} S_N^{(1)} &= \left\{\Psi_N = \sum_{m=1}^{M_1}\sum_{n=1}^{N_1} \hat{A}_{mn}\sin(amx)\sin(nz) \mid \hat{A}_{mn} \in \boldsymbol{R}\right\}, \\ S_N^{(2)} &= \left\{\Theta_N = \sum_{m=0}^{M_2}\sum_{n=1}^{N_2} \hat{B}_{mn}\cos(amx)\sin(nz) \mid \hat{B}_{mn} \in \boldsymbol{R}\right\}, \\ S_N &= S_N^{(1)} \times S_N^{(2)}, \end{aligned}$$

and denote an approximate solution of (4) by $\hat{u}_N := (\hat{\Psi}_N, \hat{\Theta}_N) \in S_N$ which is obtained by an appropriate method. Then setting

$$\begin{cases} f_1(\Psi,\Theta) & := & \sqrt{\mathcal{PR}}\,\Theta_x - \Psi_z\Delta\Psi_x + \Psi_x\Delta\Psi_z, \\ f_2(\Psi,\Theta) & := & -\sqrt{\mathcal{PR}}\,\Psi_x + \Psi_z\Theta_x - \Psi_x\Theta_z, \end{cases}$$

$$\Psi = \hat{\Psi}_N + w^{(1)}, \qquad \Theta = \hat{\Theta}_N + w^{(2)},$$

(4) is rewritten as the problem to find $(w^{(1)}, w^{(2)}) \in X^4 \times Y^2$ satisfying

$$\begin{cases} \mathcal{P}\Delta^2 w^{(1)} & = & f_1(\hat{\Psi}_N + w^{(1)}, \hat{\Theta}_N + w^{(2)}) - \mathcal{P}\Delta^2\hat{\Psi}_N & \text{in} \ \ \Omega, \\ -\Delta w^{(2)} & = & f_2(\hat{\Psi}_N + w^{(1)}, \hat{\Theta}_N + w^{(2)}) + \Delta\hat{\Theta}_N & \text{in} \ \ \Omega. \end{cases} \tag{6}$$

Note that $(w^{(1)}, w^{(2)})$ is expected to be small if $\hat{u}_N$ is an accurate approximation. Defining

$$\begin{array}{rcl} w & = & (w^{(1)}, w^{(2)}), \\ h_1(w) & = & f_1(\hat{\Psi}_N + w^{(1)}, \hat{\Theta}_N + w^{(2)}) - \mathcal{P}\Delta^2\hat{\Psi}_N, \\ h_2(w) & = & f_2(\hat{\Psi}_N + w^{(1)}, \hat{\Theta}_N + w^{(2)}) + \Delta\hat{\Theta}_N, \\ h(w) & = & (h_1(w), h_2(w)), \end{array}$$

by virtue of Sobolev embbeding theorem and the definition of f_1 and f_2, h is a bounded continuous map from $X^3 \times Y^1$ to $X^0 \times Y^0$. Moreover, it is easily shown that for all $(g_1, g_2) \in X^0 \times Y^0$, the linear problem:

$$\begin{cases} \Delta^2\bar{\Psi} & = & g_1 & \text{in} \ \ \Omega, \\ -\Delta\bar{\Theta} & = & g_2 & \text{in} \ \ \Omega \end{cases} \tag{7}$$

has a unique solution $(\bar{\Psi}, \bar{\Theta}) \in X^4 \times Y^2$. When this mapping is denoted by $\bar{\Psi} = (\Delta^2)^{-1}g_1$ and $\bar{\Theta} = (-\Delta)^{-1}g_2$, an operator:

$$\mathcal{K} := (\mathcal{P}^{-1}(\Delta^2)^{-1}, (-\Delta)^{-1}) : \ X^0 \times Y^0 \to X^3 \times Y^1$$

is a compact map because of the compactness of the imbedding $H^4(\Omega) \hookrightarrow H^3(\Omega)$, $H^2(\Omega) \hookrightarrow H^1(\Omega)$ and the boundedness of $(\Delta^2)^{-1} : X^0 \to X^4$, $(-\Delta)^{-1} : Y^0 \to Y^2$. Therefore, (6) is rewritten by a fixed-point equation:

$$w = Fw \tag{8}$$

for the compact operator $F := \mathcal{K} \circ h$ on $X^3 \times Y^1$, and Schauder's fixed-point theorem asserts that, for a nonempty, closed, bounded and convex set $W \subset X^3 \times Y^1$, if

$$FW \subset W \tag{9}$$

holds, then there exists a fixed-point of (8) in W. A concrete computer algorithm to construct a *candidate set* W which satisfies (9) is proposed in [7].

3 Numerical Examples

In the verification step, interval arithmetic is used to take account of the effects of rounding errors in the floating point computations. We use Fortran 90 library `INTLIB_90` coded by Kearfott [5] with DIGITAL Fortran V5.4-1283 on Compaq Alpha Server GS320 (Alpha 21264 731MHz; Tru64 UNIX V5.1).

3.1 The trivial solution

It is clear that the problem (4) has a trivial solution $\Psi = \Theta = 0$ for all $\mathcal{P}$ and $\mathcal{R}$. Fig.2 shows the isotherm of the temperature $T + \delta T - \frac{\delta T}{h} z$ when $T = 0$ and $\delta T = 5$.

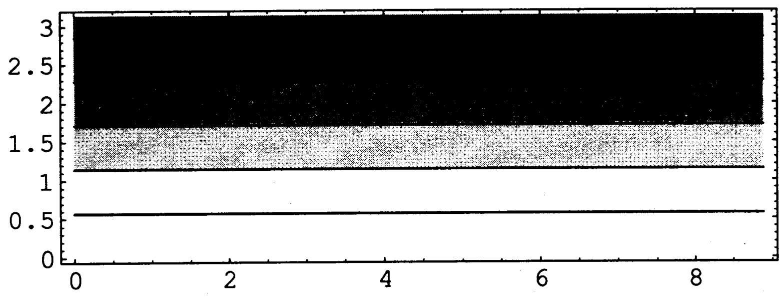

Fig.2 The isotherm of the temperature: stationary solution.

It is known that for small $\mathcal{R}$ the fluid conducts heat diffusively, and at a critial point $\mathcal{R}_C$, heat is transposed through the fluid by convection. It has been shown by Joseph [4] that (3) has a unique trivial solution for $\mathcal{R} < \mathcal{R}_C$. However, the global structure of bifurcated solutions after the critical Rayleigh point $\mathcal{R}_C$ has not been known theoretically.

3.2 First bifurcated solutions from the trivial solution

In 1916, Rayleigh [6] considered the linearized stability and found the critical Rayleigh number as follows

$$\mathcal{R}_C = \inf_{m,n} \frac{(a^2m^2 + n^2)^3}{a^2m^2} = 6.75 \quad (m = 1, n = 1, a = 1/\sqrt{2}).$$

The usual bifurcation theory implies that the stationary bifurcation occurs from the above critical point. We select $a = 1/\sqrt{2}$ and $\mathcal{P} = 10$ in the following numerical experiments. After the critical Rayleigh number $\mathcal{R}_C = 6.75$, we obtain two non-trivial approximate solutions for various Rayleigh numbers $\mathcal{R}$ of the form:

$$\hat{\Psi}_N = \sum_{m=1}^{M_1} \sum_{n=1}^{N_1} \hat{A}_{mn} \sin(amx) \sin(nz), \qquad \hat{\Theta}_N = \sum_{m=0}^{M_2} \sum_{n=1}^{N_2} \hat{B}_{mn} \cos(amx) \sin(nz)$$

for some M_1, M_2, N_1 and N_2 by Fourier-Galerkin method combined with Newton-Raphson iteration. Fig.3 shows the velocity field $(-(\hat{\Psi}_N)_z, (\hat{\Psi}_N)_x)$ at $\mathcal{R} = 50, \mathcal{P} = 10, M_1 = N_1 = M_2 = N_2 = 10$, respectively. We illustrate the particular value of coefficients, under the figures, which has the maximum absolute value in $\{\hat{A}_{mn}\}$ and $\{\hat{B}_{mn}\}$, respectively.

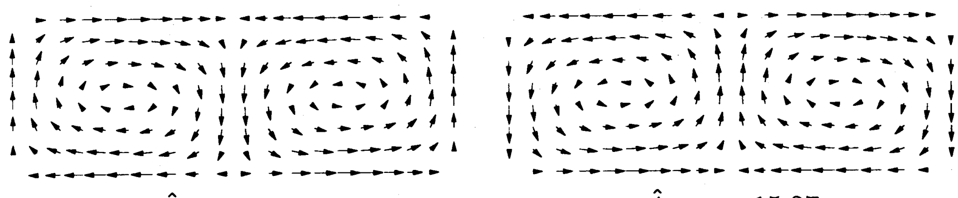

$\hat{A}_{11} \approx 15.37$ $\qquad\qquad$ $\hat{A}_{11} \approx -15.37$

Fig.3 The velocity field of the first bifurcated solution.

Fig.4 shows the isotherm of the temperature

$$\theta^* = \delta T(1 - z/\pi - \Theta/\sqrt{\mathcal{RP}}\pi) + T$$

when $T = 0$, $\delta T = 5$.

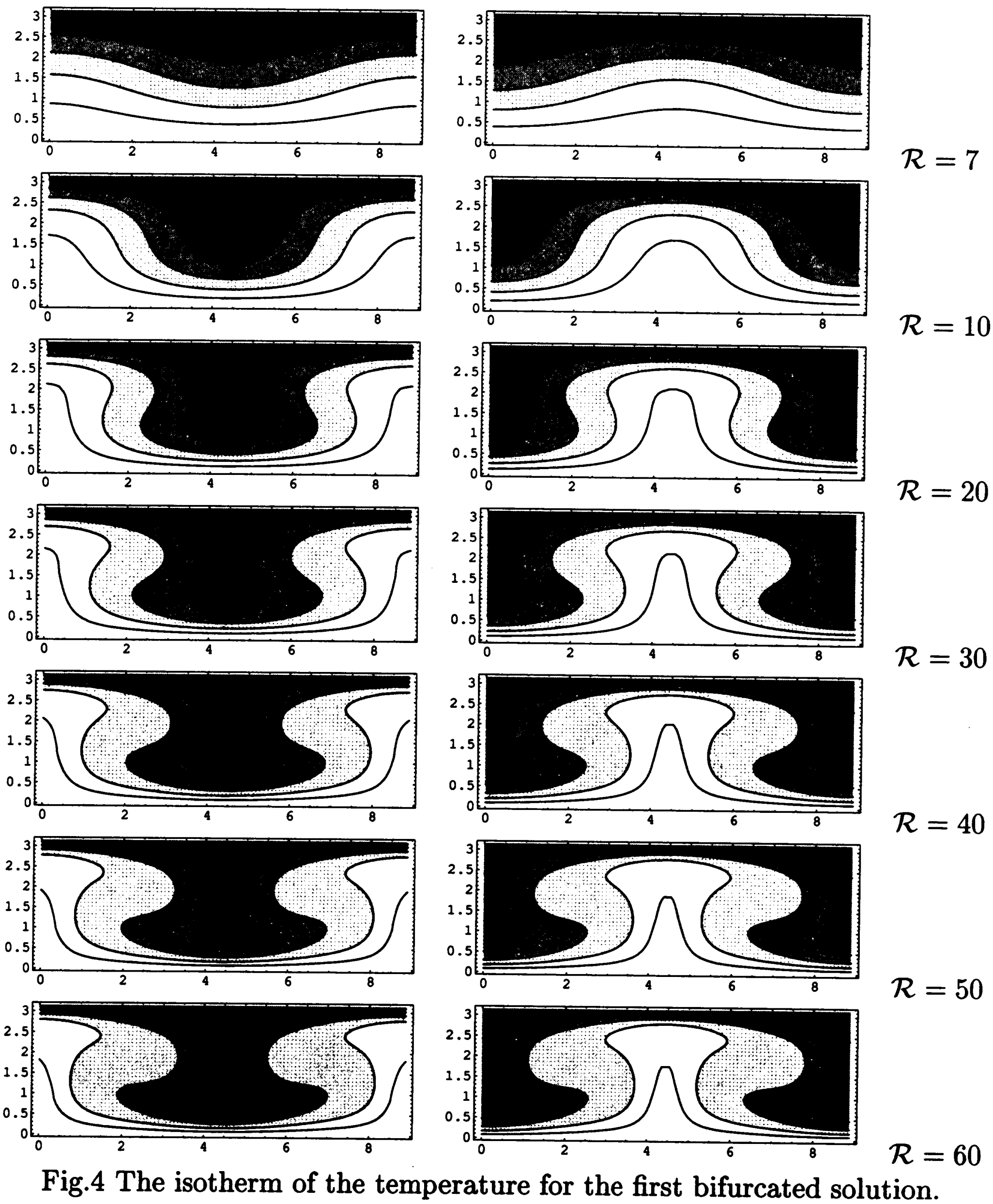

Fig.4 The isotherm of the temperature for the first bifurcated solution.

3.3 Second bifurcated solutions from the trivial solution

After the Rayleigh number

$$\mathcal{R} = \frac{(a^2m^2 + n^2)^3}{a^2m^2} = 13.5 \quad (m = 2, n = 1, a = 1/\sqrt{2}),$$

we obtain two non-trivial approximate solutions which are expected to be second bifu solutions from the trivial solution. Fig.5 and Fig.6 show the velocity field at $\mathcal{R} = 5($ $10, M_1 = N_1 = M_2 = N_2 = 10$ and the isotherm of the temperature, respectively.

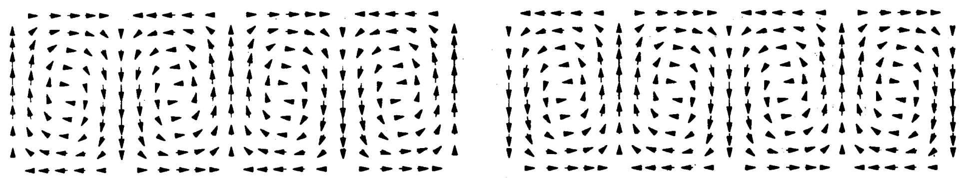

Fig.5 The velocity field of the second bifurcated solution.

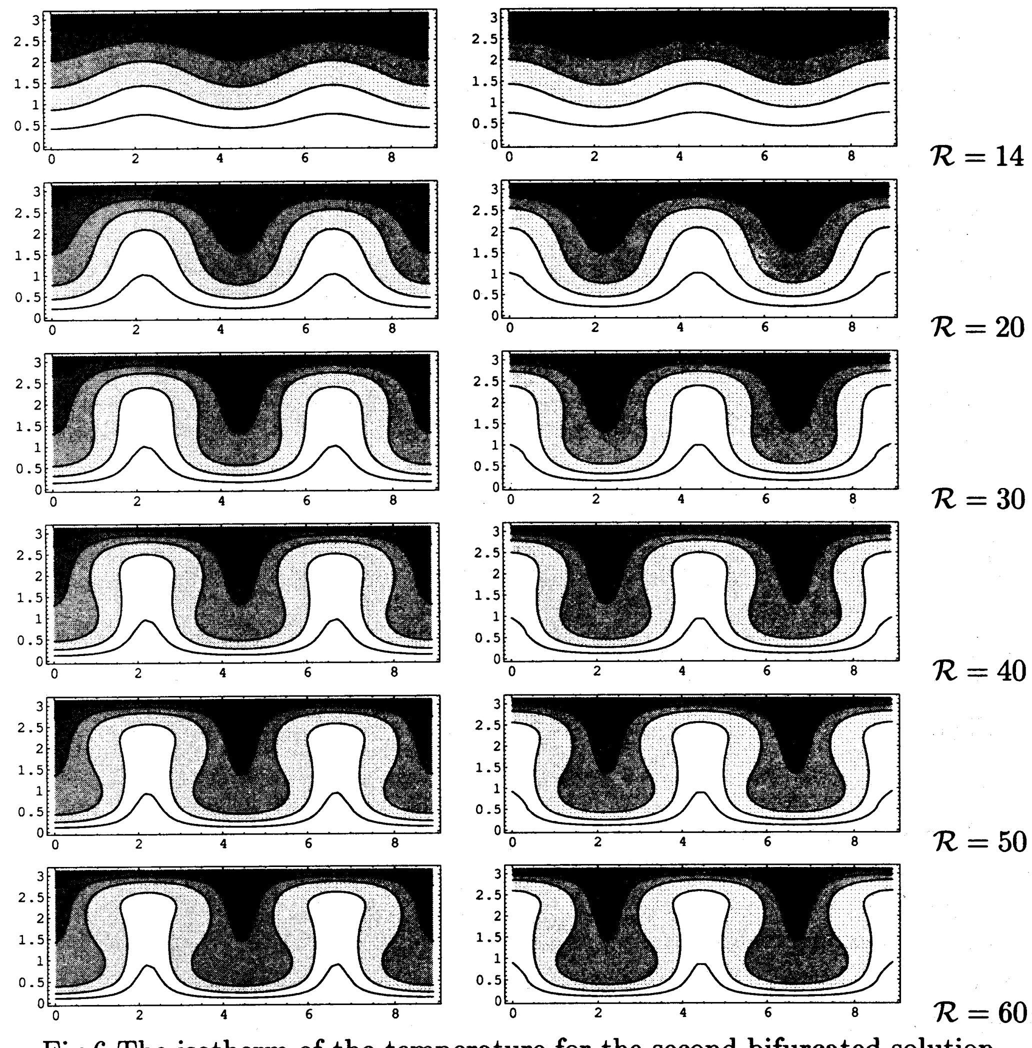

Fig.6 The isotherm of the temperature for the second bifurcated solution.

3.4 Third bifurcated solutions from the trivial solution

After the Rayleigh number

$$\mathcal{R} = \frac{(a^2m^2 + n^2)^3}{a^2m^2} = 1331/36 \quad (m = 3, n = 1, a = 1/\sqrt{2}),$$

we obtain two non-trivial approximate solutions which are expected to be third bif solutions from the trivial solution. Fig.7 and Fig.8 show the velocity field at $\mathcal{R} =$ 10, $M_1 = N_1 = M_2 = N_2 = 10$ and the isotherm of the temperature, respectively.

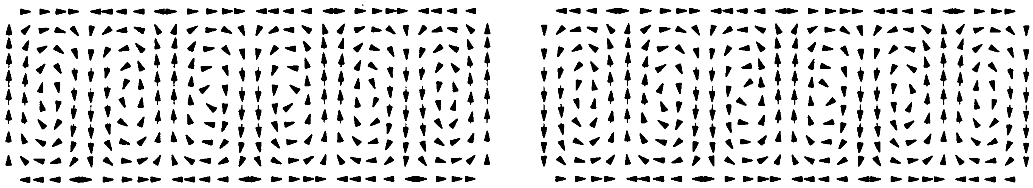

$\hat{A}_{31} \approx -2.029$ $\hat{A}_{31} \approx 2.029$

Fig.7 The velocity field of the third bifurcated solution.

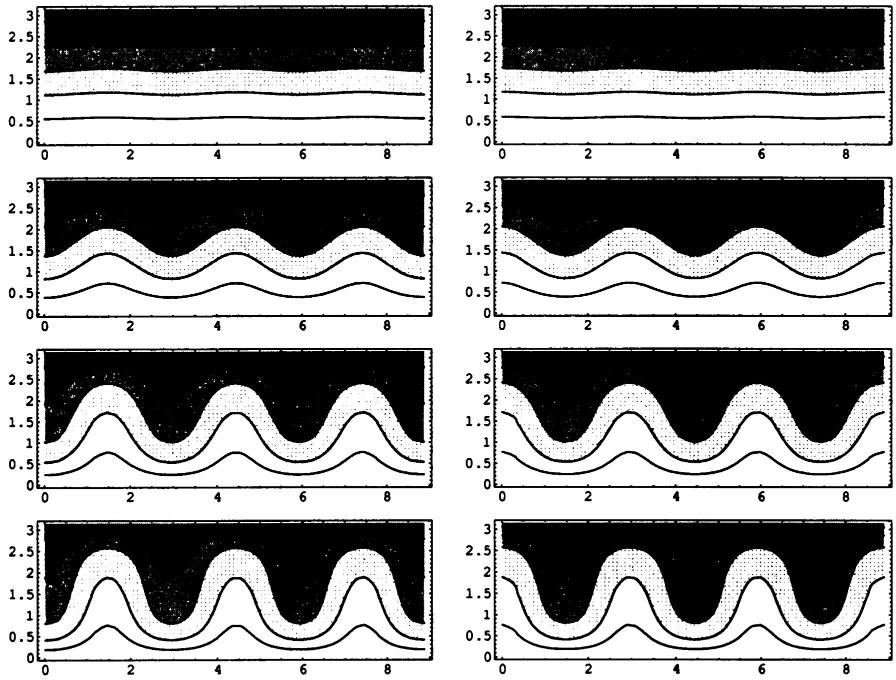

$\mathcal{R} = 37$

$\mathcal{R} = 40$

$\mathcal{R} = 50$

$\mathcal{R} = 60$

Fig.8 The isotherm of the temperature for the third bifurcated solution.

3.5 Another non-trivial solutions

We also obtain four different non-trivial approximate solutions after $\mathcal{R} = 32.5$. According to this observation, we expected the existence of another bifurcated solutions from the non-trivial solutions which seem to be on the second bifurcation branch (cf.Fig.11). For example, we observed the phenomena as shown in Fig.9 and Fig.10 for the case that $\mathcal{R} = 50, \mathcal{P} = 10, M_1 = N_1 = M_2 = N_2 = 10$.

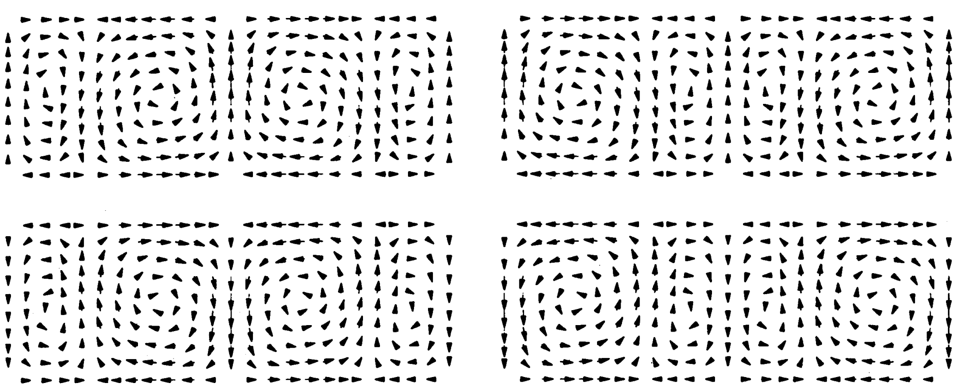

Fig.9 The velocity field of the another non-trivial solutions.

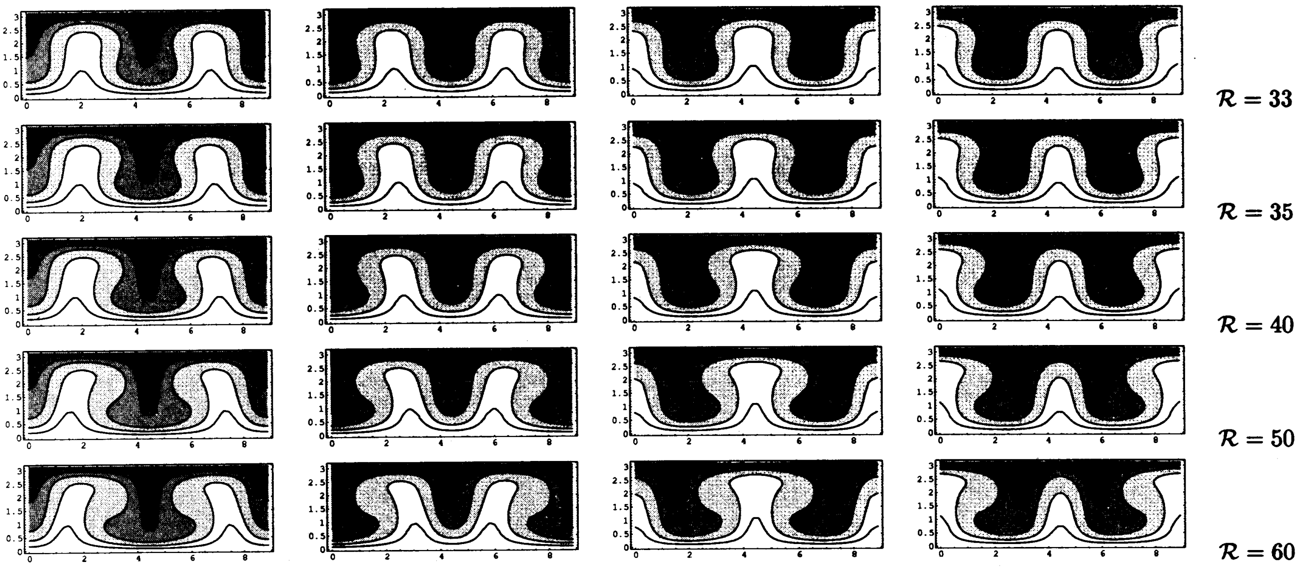

Fig.10 The isotherm of the temperature for the another non-trivial solutions.

3.6 Verification Results

We actually succeeded to verify the exact solutions of (4) corresponding to the approximate solutions in Fig.9 and Fig.10, as in Fig.11. The vertical axis shows the absolute value of the coefficient of the approximate solution: $\hat{\Theta}_N = \sum_{m=0}^{M_2} \sum_{n=1}^{N_2} \hat{B}_{mn} \sin(amx) \sin(nz)$. Each dot implies that the verification procedure are succeeded.

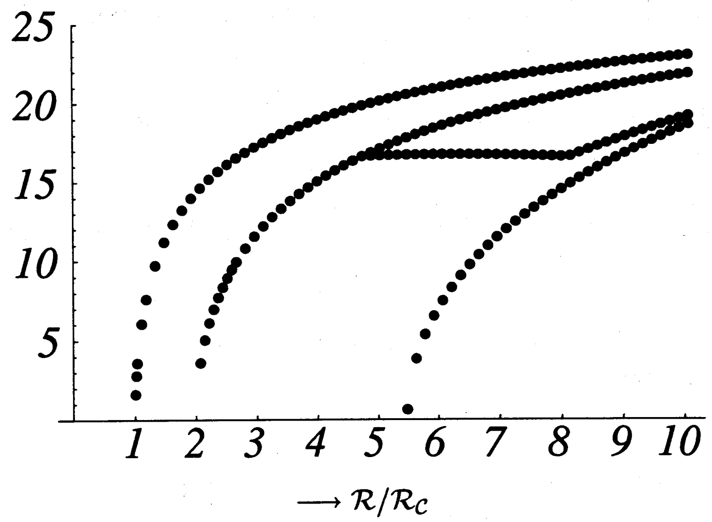

Fig.11 The bifurcation curve.

Table 1 shows the error bounds when $\mathcal{R} = 60$, $\mathcal{P} = 10$, $N := M_1 = M_2 = N_1 = N_2$. There exist the solution $(\Psi, \Theta) \in X^3 \times Y^1$ of (4) in

$$\Psi \in \hat{\Psi}_N + W_N^{(1)} + W_*^{(1)},$$
$$\Theta \in \hat{\Theta}_N + W_N^{(2)} + W_*^{(2)}.$$

Table 1. Verification results; $\mathcal{R} = 60$, $\mathcal{P} = 10$

$No.$	N	$\|\hat{\Psi}_N\|_{L^2}$	$\|\hat{\Theta}_N\|_{L^2}$	$\|W_N^{(1)}\|_{L^\infty}$	$\|W_N^{(2)}\|_{L^\infty}$	$\|W_*^{(1)}\|_{L^\infty}$	$\|W_*^{(2)}\|_{L^\infty}$
1	45	17.44	34.89	1.40×10^{-9}	3.12×10^{-11}	2.46×10^{-11}	1.26×10^{-7}
2	45	17.44	34.89	1.40×10^{-9}	3.12×10^{-11}	2.46×10^{-11}	1.26×10^{-7}
3	30	8.14	30.57	2.35×10^{-6}	2.56×10^{-8}	7.75×10^{-8}	1.35×10^{-4}
4	30	8.14	30.57	2.35×10^{-6}	2.56×10^{-8}	7.75×10^{-8}	1.35×10^{-4}
5	50	9.62	29.43	9.75×10^{-9}	8.77×10^{-10}	6.96×10^{-11}	5.21×10^{-7}
6	50	9.62	29.43	9.75×10^{-9}	8.77×10^{-10}	6.96×10^{-11}	5.21×10^{-7}
7	50	9.62	29.43	9.75×10^{-9}	8.77×10^{-10}	6.96×10^{-11}	5.21×10^{-7}
8	50	9.62	29.43	9.75×10^{-9}	8.77×10^{-10}	6.96×10^{-11}	5.21×10^{-7}
9	20	2.84	19.49	3.40×10^{-5}	9.56×10^{-7}	1.75×10^{-6}	1.10×10^{-3}
10	20	2.84	19.49	3.40×10^{-5}	9.56×10^{-7}	1.75×10^{-6}	1.10×10^{-3}

From our verification results we cannot decide whether the verified solutions are really bifurcated or simply isolated solutions. We also cannot say for certain whether the verified solutions are continuous for the Rayleigh number or locally unique in the candidate sets. These questions must be solved in our future works.

参考文献

[1] Chandrasekhar, S.: *Hydrodynamic and Hydromagnetic Stability*, Oxford University Press, 1961.

[2] Curry, J. H.: Bounded solutions of finite dimensional approximations to the Boussinesq equations, *SIAM J. Math. Anal.* **10**, pp.71–79 (1979).

[3] Getling, A. V.: *Rayleigh-Bénard Convection: structures and dynamics*, Advanced series in nonlinear dynamics Vol.11, World Scientific, 1998.

[4] Joseph, D. D.: On the stability of the Boussinesq equations, *Arch. Rational Mech. Anal.* **20**, pp.59–71 (1965).

[5] Kearfott, R. B., and Kreinovich, V., *Applications of Interval Computations*, Kluwer Academic Publishers, Netherland, 1996.
(`http://interval.usl.edu/kearfott.html`)

[6] Rayleigh, J. W. S.: On convection currents in a horizontal layer of fluid, when the higher temperature is on the under side, *The London, Edinburgh and Dublin Philosophical Magazine and Journal of Science, Ser.6*, Vol.32, pp.529–546 (1916); and *Scientific Papers*, Vol.6, pp.432–446 (1920).

[7] 渡部 善隆, 中尾 充宏, 山本 野人, 西田 孝明: Rayleigh-Bénard 対流の定常解に対する精度保証付き数値計算, 短期共同研究・精度保証付き数値計算法とその周辺, 京都大学数理解析研究所講究録, Vol.1147 (2000) pp.132–136.